HUMAN BODY MODELING IN THE VICINITY OF HIGH VOLTAGE TRANSMISSION LINES

Alireza Fereidouni [1], Behrooz Vahidi[2*], Farnaz Shishehgar[3], Tahoura Hosseini Mehr[1], Mahdi Tahmasbi[1]
1- Young Researchers and Elite Club, Neka Branch, Islamic Azad University, Neka, Iran
2-Department of Electrical Engineering, Amirkabir University of Technology, Tehran 1591634311, Iran
3-Department of Nursing and Midwifery, Islamic Azad University, Tehran Medical Branch, Tehran, Iran
* Corresponding author email: vahidi@aut.ac.ir

ABSTRACT: *Interactions of electric and magnetic fields at power line frequencies (50 and 60 Hz) in humans have been the subject of intensive scientific inquiry and considerable public concern during the last two decades. As a part of the scientific effort, extensive evaluations of induced electric field and current density in the human body have been performed. Realistic, heterogeneous, high-resolution models of the body have been analyzed using various numerical methods. For this reason, this paper investigates the induced currents in the human body organs (such as brain, heart, and kidney) and on the surface of it (skin) when exposed to a 200 kV transmission line (TL) 50 Hz. Hence, firstly, a numerical method has been employed to calculate the induced currents in the organs and on the surface of the body. Secondly, A test object which can represent the human body in experiments near energized high-voltage (HV) conductors has been developed. All in all, in this paper, it is aimed to obtain the induced current level changes of the human body due to its distances (0, 5, 10, 15, and 20 meter) from the center of an energized high-voltage transmission line. The numerical results present a good agreement in compare with the experimental results.*

Keywords: Human model, electric field, magnetic field, transmission line and induced current.

NOMENCLATURE

u_x	The unit vector along the X axis
u_y	The unit vector along the Y axis
u_z	The unit vector along the Z axis
B_{0x}	The amplitude of magnetic field in the X direction
B_{0y}	The amplitude of magnetic field in the Y direction
B_{0z}	The amplitude of magnetic field in the Z direction
E	Electric field
D	Displacement current
B	Magnetic flux
H	Magnetic field
J	Current density
ρ	Volume charge density
σ	Effective conductivity
μ	Permeability
J_0	Source current
ε	Permittivity
ω	Angular frequency

1. INTRODUCTION

Electrical energy can be taken into account vital for all places of society, industrial, domestic, and social, in such a way that it is hard to assume a human activity that does not have some relationship with electricity. Electrical Energy is transferred from the power station to the substation through high-voltage (HV) transmission lines (TLs) and from there to the final users through distribution grids of medium and low voltage [1-2].

Public concerns about power-frequency fields first emerged in the late 1960s as power companies turned increasingly to HV transmission lines to handle large increases in electricity use. HV lines carry electric power with lower energy losses and with smaller land usage than multiple lower-voltage lines with the same power-delivery capacity. Public attention to HV transmission lines focused first on the aesthetic impact of their large towers, on the aesthetic and ecological impacts of their rights-of-way, and on various nuisance effect created by their strong electric fields. This nuisance effect include audible noise, TV/radio interference, and induced shocks that can occur when a person standing beneath an HV line touches a large ungrounded metal object such as a truck or farm vehicle.

By the early 1970s, the American national standards institute (ANSI) had issued voluntary standards to address nuisance effect. The first evidence that power-frequency fields might have a direct effect on human health appeared in 1972 when Soviet investigators reported that workers in Soviet HV switchyards suffered from a number of non-specific ailments [3]. Although these reports were greeted with much skepticism by western scientists, they served to stimulate public concern. By the mid-seventies, health effect had become acentral issue in transmission line in several states. The issues have been investigating until now.

Overhead line workers (linesmen) become exposed to high electric and magnetic fields on a regular basis as a result of working close to HV transmission lines. These fields can cause induced currents and voltages. The electric fields induce currents on the body surface while the magnetic fields induce internal body currents [4]. The capacitance coupling the body to the HV lines combined with its capacitance to ground dictates the induced voltage levels. The work reported here considers the short-term impact on linesmen resulting from the electric fields. Routine checks and inspections of overhead transmission lines are performed by linesmen during non-outage conditions. A typical task which exposes them to electric fields is tower condition assessment where linesmen climb a 200-kV tower to its peak while maintaining the safety distances to the live conductors. These conditions occasionally lead linesmen to experience unpleasant discharges that may reach levels that require them to put off their working activity.

For this reason, this paper aims to calculate the induced currents in the organs of a human body such as brain, heart, kidney and also on the surface of it (skin) while he is working under a 200 kV TL 50 Hz. This goal has been reached by:

- Analytically calculating the incident electromagnetic field surrounding a typical 200 kV transmission line,
- Numerically calculating the induced currents in the human organs (brain, heart, kidney, and skin) produced by the incident electromagnetic field, and
- Experimentally obtaining the induced currents in the human organs (brain, heart, kidney, and skin) produced by the incident electromagnetic field in the HV laboratory.

Numerical methods are often employed to determine the field distributions within or around a human body from realistic electromagnetic sources. With detailed anatomical models [5], induced fields within a human body can be computed with greater resolution. In this paper, a numerical technique based on the finite element method (FEM) [6] and electromagnetic quasi-static approximations is applied in the analysis of low frequency electromagnetic exposure to human body. For verifying the numerical results, an experimental test has been carried out. A simplified 3-D test object has been designed to represent the human body in experiments that took place inside the HV laboratory. This experiment aims to examine how the induced current levels of a test object change according to its distance from an energized overhead line and a relatively large grounded object such as a 3 m tall tower placed inside the laboratory. This means that a human model which includes the human organs in it has been developed and located under an energized conductor for measuring the induced currents. Note that because the human organs could not be prepared, the organs of a sheep have been used. The numerical results show a good agreement with the experimental measurements.

2. The Electromagnetic Field of Transmission Lines

2.1. Definition

The HV transmission line system, part of the power network, includes the huge generating plants that gather power through hydroelectric processes, like Niagara Falls, through the burning of fossil fuels like oil and coal, or through nuclear fission at nuclear-power plants [7]. The voltage form of these plants is shortly raised in step-up transformers and is moved along HV transmission lines strung on tall, specially designed towers. When it arrives the community where it is needed, the voltage is decreased in step-down transformers in power substations. The energy can then be used by final users (such as houses and industries) through the distribution grid.

There are various configurations of HV overhead power transmission lines. Typical three-phase, three-wire (conductor) power lines can be arranged horizontally, vertically or equilaterally (Figure 1) [7]. In this paper, horizontal configuration will be considered. This type which is a 200 kV TL is depicted in Figure 2 (case study). The information of this TL is given in Table 1.

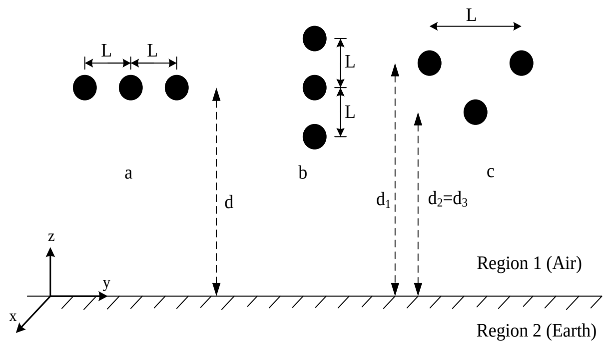

Figure 1. Three-phase transmission lines; (a) horizontal, (b) vertical, and (c) equilateral arrangements.

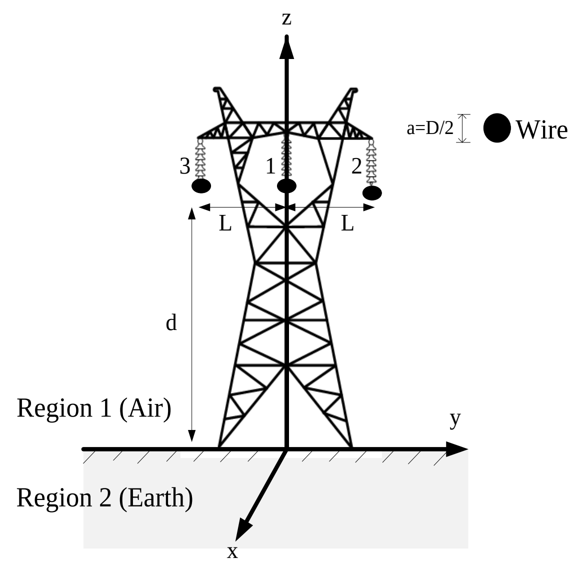

Figure 2. Schema of a 200 kV TL at the height of d over the earth (case study).

TABLE 1
INFORMATION OF THE UNDER STUDIED OVERHEAD TL (200 kV-50 Hz)

Parameters	L (meter)	d (meter)	I (Ampere)	f (Hz)	a (meter)
200 kV TL	3	15	300	50	0.012

2.2. The Formulation

The sources of electrical and magnetic fields in the environment of TLs are the electrical currents and charges that exist in their conductors, as well as those which are induced in the earth and/or in nearby objects. The starting points for the calculation of these variable fields with time are Maxwell's equations [2-3].

Generally, electrical and magnetic fields are coupled, and it is essential to solve Maxwell's equations to acquire them. Some authors [8-15] have suggested models that solve Maxwell's equations to obtain the value from the magnetic field generated by TLs. In practical terms, these models are not the most suitable for the calculation of the magnetic field in the proximity of TLs due to their complex math. Thanks to this, a simpler mathematical model, but one that represents similar results to the real values, will be more useful. Though the electromagnetic fields generated by TLs are coupled, in many cases and under certain conditions, some approximations can be assumed and electromagnetic fields calculated in an independent way. This is often the case for fields created by TLs because of the fact that the field changes so slowly in time that Maxwell's equations are altered into the electro-static and magneto-static equations.

In figure 2 the central conductor (1) is in the plane $y=0$, while conductors (2) and (3) are respectively in the planes $y=L$ and $y=-L$. Three conductors in the plan $z=d$ are in the air ($\text{Region } 0$) above the surface $z=0$ of the earth ($\text{Region } 1$). The analytical formulas for field calculations of the three phase's power system are derived in [8]. As shown in figure 2, this type of transmission line has three horizontal conductors that the magnitudes of the currents of three conductors are the same, and they differ in phase according to:

$$\left|I_1(x)\right| = \left|I_2(x)\right| = \left|I_3(x)\right|$$

$$I_a(x) = I_a(x)e^{j0}$$

$$I_b(x) = I_a(x)e^{j2\pi/3}$$

$$I_c(x) = I_a(x)e^{-j2\pi/3}$$

The total current crossing a plane $x = \text{constatnt}$ is as follow:

$$I(x) = I_1(x) + I_2(x) + I_3(x) =$$

$$I_1(x)\left[1 + e^{i2\pi/3} + e^{-i2\pi/3}\right]$$

$$= I_1(x)\begin{bmatrix} 1 + 2\cos(2\pi/3) + \\ i\sin(2\pi/3) - i\sin(2\pi/3) \end{bmatrix} = 0$$

The three components of the electric field in the cylindrical coordinates ρ, φ, z of horizontal electric dipole with the electric moment $I dx$ at a height d in air over a plane earth are given in [8]. The corresponding formulas in rectangular coordinates are readily derived. The field of the power line when this is terminated to maintain a traveling wave with the form $I_1(x') = I_1(0)e^{ik_0x'}$ is acquired from the formulas for the dipole with the substitution of $x - x'$ for x. When this substitution has been performed, the field in the plane $x=0$ due to all three conductors is as follow:

$$[E_{0j}(0,y,z)]_t = \int_{-\infty}^{\infty}[E_{0j}(0,y,z) + e^{i2\pi/3}E_{0j}(0,y+L,z) + e^{-i2\pi/3}E_{0j}(0,y-L,z)] \times e^{ik_0x'}dx'$$

$$j = x, y, z$$

Since the field of any element $I(x')dx'$ of the three-wire line decreases rapidly with distance from $x = x'$, the limits of integration have been altered from a very large distance in each direction to $\pm\infty$. The relevant rectangular components of the electric field are:

$$E_{0x}(0,y,z) = \frac{i\omega\mu_0 I}{\pi k_1^2}(k_0 d)\left\{\frac{(z+d)^2 - y^2}{\left[(z+d)^2 + y^2\right]^2} + e^{i\frac{2\pi}{3}}\left[\frac{(z+d)^2 - (y+L)^2}{\left[(z+d)^2 + (y+L)^2\right]^2}\right] + e^{-i\frac{2\pi}{3}}\left[\frac{(z+d)^2 - (y-L)^2}{\left[(z+d)^2 + (y-L)^2\right]^2}\right]\right\}$$

$$E_{0y}(0,y,z) = \frac{\omega\mu_0 I}{2\pi k_0}\left\{\begin{array}{l} y\left[\dfrac{1}{(z-d)^2 + y^2} - \dfrac{1 - \dfrac{2k_0^2}{k_1^2}}{(z+d)^2 + y^2}\right] + e^{i\frac{2\pi}{3}}(y+L)\left[\dfrac{1}{(z-d)^2 + (y+L)^2} - \dfrac{1 - \dfrac{2k_0^2}{k_1^2}}{(z+d)^2 + (y+L)^2}\right] \\ + e^{-i\frac{2\pi}{3}}(y-L)\left[\dfrac{1}{(z-d)^2 + (y-L)^2} - \dfrac{1 - \dfrac{2k_0^2}{k_1^2}}{(z+d)^2 + (y-L)^2}\right] \end{array}\right\}$$

$$E_{0z}(0,y,z)=\frac{\omega\mu_0 I}{2\pi k_0}\left\{\begin{aligned}&\frac{z-d}{(z-d)^2+y^2}-\frac{z+d}{(z+d)^2+y^2}+e^{i\frac{2\pi}{3}}\left[\frac{z-d}{(z-d)^2+(y+L)^2}-\frac{z+d}{(z+d)^2+(y+L)^2}\right]\\&+e^{-i\frac{2\pi}{3}}\left[\frac{z-d}{(z-d)^2+(y-L)^2}-\frac{z+d}{(z+d)^2+(y-L)^2}\right]\end{aligned}\right\}$$

To determined components of magnetic field use is made of Maxwell's equation:

$$j\omega B(x,y,z)=\nabla\times E(x,y,z) \qquad (10)$$

On HV overhead transmission lines, the load is held constant so that the power flow is mostly a forward traveling wave. In this paper, only the forward-traveling field is considered. Referred to the central plane through the body defined by $x=0$, the traveling-wave incident field is $E(x,y,z)=E(0,y,z)e^{jk_0x}$ so that:

The components of fields are:

$$j\omega B_{0x}(0,y,z)=\frac{\partial}{\partial y}E_{0z}(0,y,z)-\frac{\partial}{\partial z}E_{0y}(0,y,z) \qquad (11)$$

$$j\omega B_{0y}(0,y,z)=\frac{\partial}{\partial z}E_{0x}(0,y,z)-jk_0E_{0z}(0,y,z) \qquad (12)$$

$$j\omega B_{0z}(0,y,z)=jk_0E_{0y}(0,y,z)-\frac{\partial}{\partial y}E_{0x}(0,y,z) \qquad (13)$$

Where:

$$\partial E(x,y,z)/\partial t=jk_0E(0,y,z)e^{jk_0x} \qquad))$$

$$B_{0x}(0,y,z)=-\frac{2ik_0\mu_0 I}{\pi k_1^2}\left\{\frac{y(z+d)}{\left[(z+d)^2+y^2\right]^2}+e^{i\frac{2\pi}{3}}\left[\frac{(y+L)(z+d)}{\left[(z+d)^2+(y+L)^2\right]^2}\right]+e^{-i\frac{2\pi}{3}}\left[\frac{(y-L)(z+d)}{\left[(z+d)^2+(y-L)^2\right]^2}\right]\right\} \qquad) \qquad ($$

$$B_{0y}(0,y,z)=\frac{\mu_0 I}{2\pi}\left\{\begin{aligned}&\frac{4(z+d)(k_0d)}{k_1^2[(z+d)^2+y^2]^2}\left[1-\frac{2[(z+d)^2-y^2]}{(z+d)^2+y^2}\right]-\frac{z-d}{(z-d)^2+y^2}+\frac{z+d}{(z+d)^2+y^2}+e^{i\frac{2\pi}{3}}\Big[\frac{4(z+d)(k_0d)}{k_1^2[(z+d)^2+(y+L)^2]^2}\\&\times\left[1-\frac{2[(z+d)^2-(y+L)^2]}{(z+d)^2+(y+L)^2}\right]-\frac{z-d}{(z-d)^2+(y+L)^2}+\frac{z+d}{(z+d)^2+(y+L)^2}\Big]+e^{-i\frac{2\pi}{3}}\Big[\frac{4(z+d)(k_0d)}{k_1^2[(z+d)^2+(y-L)^2]^2}\\&\times\left[1-\frac{2[(z+d)^2-(y-L)^2]}{(z+d)^2+(y-L)^2}\right]-\frac{z-d}{(z-d)^2+(y-L)^2}+\frac{z+d}{(z+d)^2+(y-L)^2}\Big]\end{aligned}\right\} \qquad ($$

$$B_{0z}(0,y,z)=\frac{\mu_0 I}{2\pi}\left\{\begin{aligned}&\frac{4(y)(k_0d)}{k_1^2[(z+d)^2+y^2]^2}\left[1+\frac{2[(z+d)^2-y^2]}{(z+d)^2+y^2}\right]+\frac{y}{(z-d)^2+y^2}-\frac{y[1-2\frac{k_0^2}{k_1^2}]}{(z+d)^2+y^2}+e^{i\frac{2\pi}{3}}\Big[\frac{4(y+L)(k_0d)}{k_1^2[(z+d)^2+(y+L)^2]^2}\\&\Big[1+\frac{2\left[(z+d)^2-(y+L)^2\right]}{(z+d)^2+(y+L)^2}\Big]+\frac{(y+L)}{(z-d)^2+(y+L)^2}-\frac{(y+L)[1-2\frac{k_0^2}{k_1^2}]}{(z+d)^2+(y+L)^2}\Big]+e^{-i\frac{2\pi}{3}}\Big[\frac{4(y-L)(k_0d)}{k_1^2[(z+d)^2+(y-L)^2]^2}\\&\left[1+\frac{2\left[(z+d)^2-(y-L)^2\right]}{(z+d)^2+(y-L)^2}\right]+\frac{(y-L)}{(z-d)^2+(y-L)^2}-\frac{(y-L)[1-2\frac{k_0^2}{k_1^2}]}{(z+d)^2+(y-L)^2}\Big]\end{aligned}\right\} \qquad ($$

In the above formulas, k_0 and k_1 are the wave number of the air and the wave number of the earth respectively. Note that, HV transmission lines have frequency equal to 50 Hz, therefore at this extremely low frequency, $\sigma_1/\omega\varepsilon_1\varepsilon_0\approx 1$ (σ_1 the conductivity and ε_1 the relative permittivity of the earth) so that k_1 reduces to the form given. If the earth is covered with a layer of asphalt or concrete, this is electrically so thin at $f=50\,\mathrm{Hz}$, that its presence has no discernible impact on the field in the air.

The maximum electromagnetic fields for a 200 kV (Figure 2, and Table. 1) are shown analytically in Figure 3 at distances 0, 2, 4, 6, 8, 10, 12, and 20 meters starting from the earth ($z=0,\ 2$ to 20).

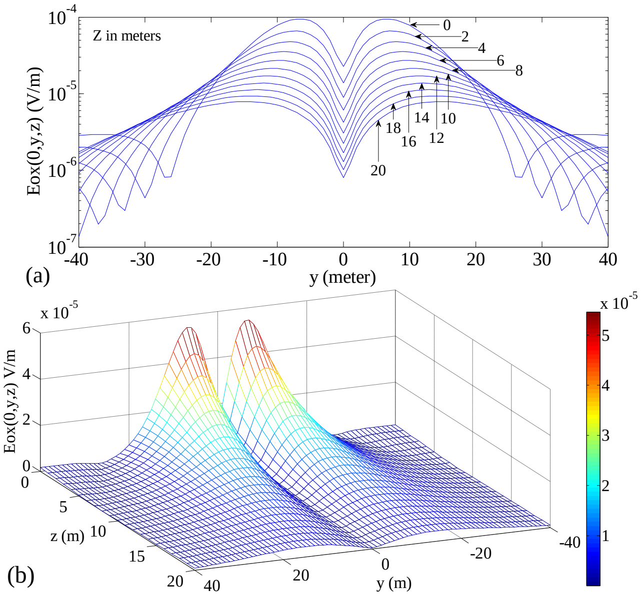
Z in meters
Eox(0,y,z) (V/m)
y (meter)
(a)
Eox(0,y,z) V/m
z (m)
y (m)
(b)
(1)

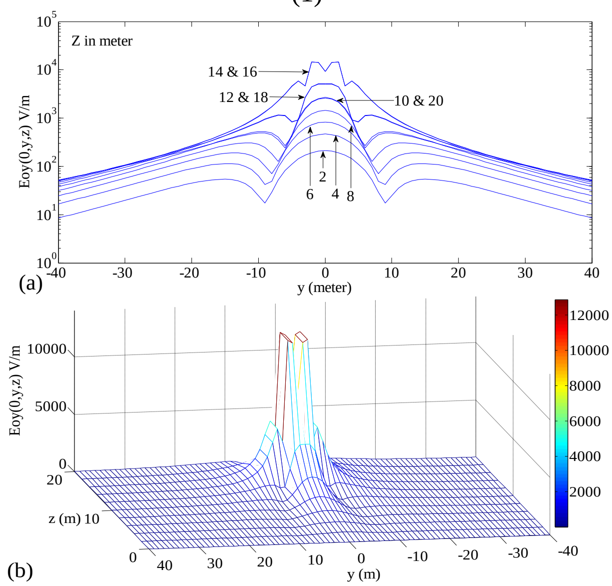
Z in meter
Eoy(0,y,z) V/m
14 & 16
12 & 18
10 & 20
y (meter)
(a)
Eoy(0,y,z) V/m
z (m)
y (m)
(b)
(2)

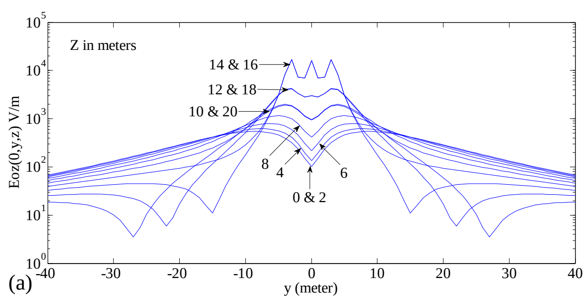
Z in meters
Eoz(0,y,z) V/m
14 & 16
12 & 18
10 & 20
0 & 2
y (meter)
(a)

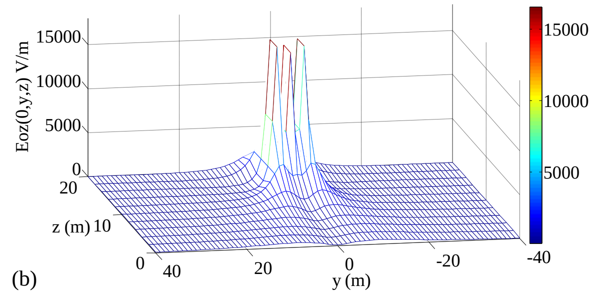
Eoz(0,y,z) V/m
z (m)
y (m)
(b)
(3)

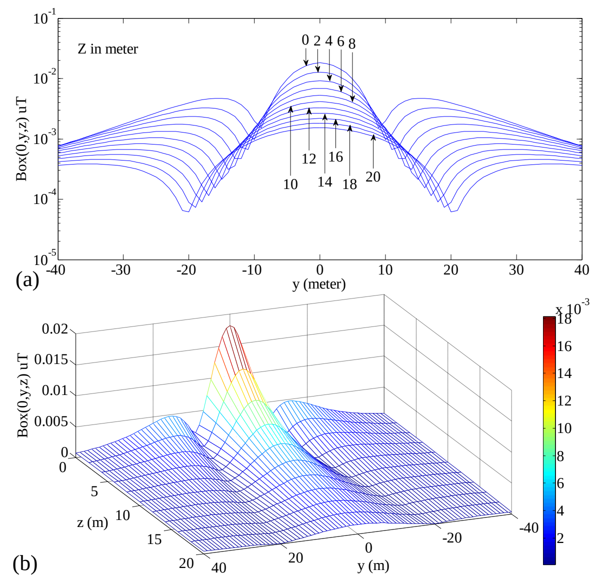
Z in meter
Box(0,y,z) uT
y (meter)
(a)
Box(0,y,z) uT
z (m)
y (m)
(b)
(4)

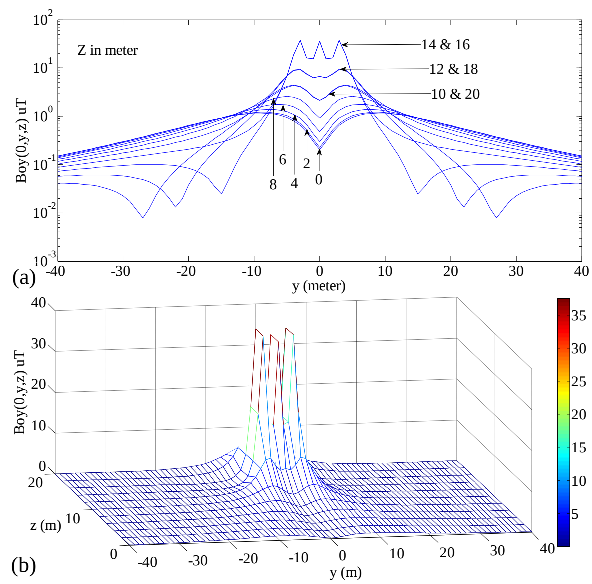
Z in meter
Boy(0,y,z) uT
14 & 16
12 & 18
10 & 20
y (meter)
(a)
Boy(0,y,z) uT
z (m)
y (m)
(b)
(5)

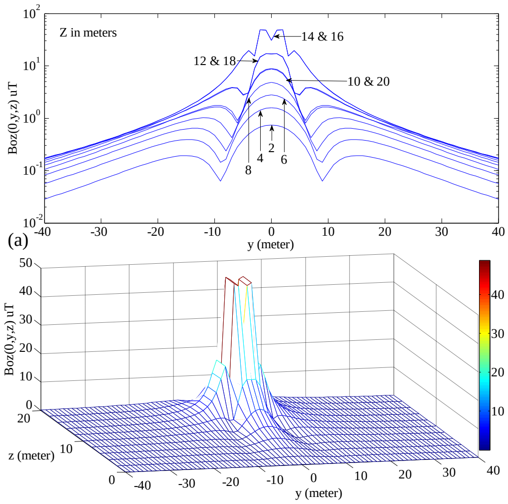

Figure 3. The electromagnetic field near a 200 kV three-wire power line over vertical distances from 0 to 20 m in 2-D and 3-D views, (1) $E_{ox}(0, y, z)$, (2) $E_{oy}(0, y, z)$, (3) $E_{oz}(0, y, z)$, (4) $B_{ox}(0, y, z)$, (5) $B_{oy}(0, y, z)$, and (3) $B_{oz}(0, y, z)$.

3. INDUCED CURRENT IN THE HUMAN BODY

3.1. Numerical Method (Simulation Method)

Maxwell's equations can be represented in complex phasor form [6]:

$$\nabla \times E = -j\omega B \qquad 4)$$

$$\nabla \times H = j\omega D + J \qquad 5)$$

$$\nabla . D = \rho \qquad 6)$$

$$\nabla . B = 0 \qquad 7)$$

Three constitutive laws govern the electromagnetic theory together with the Maxwell's equations [8]:

$$D = \varepsilon E \qquad 8)$$

$$B = \mu H \qquad 9)$$

$$J = \sigma E + J_0 \qquad 0)$$

The quasi-static laws are obtained from the Maxwell's equations by neglecting either the magnetic induction or the electric displacement current. To justify the quasi-static approximations, one has to ensure that neglecting the magnetic induction in EQS or the displacement current in MQS does not make significant error. For a characteristic length d, the condition $\omega^2 \mu d^2 \tilde{\varepsilon} \ll 1$ must be satisfied by all materials within the computation domain. Assume a vector potential A where $\nabla \times A = B$ and a scalar electric potential ϕ_e, Electric field can be represented as [16]:

$$E = \nabla \phi_e - j\omega A \qquad 1)$$

Apply the EQS or the MQS approximation; two equations can be obtained as [16]:

$$\nabla . \tilde{\varepsilon} \nabla \phi_e = j\omega \nabla . \tilde{\varepsilon} A \qquad 2)$$

$$\nabla . \tilde{\varepsilon} \nabla \phi_e = 0 \qquad 3)$$

If all the materials depict dielectric properties that obey $\sigma \approx \omega\varepsilon$, so it can be written:

$$\nabla . \sigma \nabla \phi_e = j\omega \nabla . \sigma A \qquad 4)$$

The vector potential A is equivalent to the magneto-static vector potential A_0 which is totally decoupled from the electric field. If the permeability μ is constant over the entire computation domain, A_0 can be calculated by the Biot-Savart law [16]:

$$\nabla . \tilde{\varepsilon} \nabla \phi_e = j\omega \nabla . \tilde{\varepsilon} A \qquad 5)$$

$$\nabla . \tilde{\varepsilon} \nabla \phi_e = 0 \qquad 6)$$

If all the materials depict dielectric properties that obey $\sigma \approx \omega\varepsilon$, so it can be written:

$$\nabla . \sigma \nabla \phi_e = j\omega \nabla . \sigma A \qquad 7)$$

The vector potential A is equivalent to the magneto-static vector potential A_0 which is totally decoupled from the electric field. If the permeability μ is constant over the entire computation domain, A_0 can be calculated by the Biot-Savart law [16]:

$$A_0(r) = \frac{\mu}{4\pi} \int_{\Omega} \frac{J_0(r')}{|r - r'|} dr' \qquad 8)$$

The electromagnetic fields can be calculated by solving Eq. (27) for the EQS case, and solving Eq. (28) and (29) for the MQS case, respectively. The partial differential equations can be solved efficiently by Finite Element Method [16-17] and using 3D Cartesian grids. In this research, as depicted in Figure 4, a human body model of a male from the "Virtual Family" package is utilized.

CAD model:

high resolution MRI scan

200 organs and 80 tissue types

Figure 4. Anatomical human body of a male.

The dielectric properties of biological tissues vary substantially dependent to frequency. In low frequency range, biological tissues are chiefly diamagnetic ($\mu = \mu_0$), and exhibit high relative permittivity and low conductivity. The tissue conductivity and permittivity values utilized in this paper are acquired from [17-19]. A list of tissue dielectric properties at 50 Hz for some of the tissues used in the study is given in Table 2.

TABLE 2.

RELATIVE CONDUCTIVITY (σ) AND PERMITTIVITY (ε_r) VALUES OF TISSUES [19]

Tissue	Fat	Muscle	Bone	Heart	Kidney	Brain	Liver

ε_r	1.14×10^{6}	1.77×10^{7}	8867.8	8.66×10^{6}	1.01×10^{7}	5.29×10^{6}	1.83×10^{6}
$\sigma(S/m)$	0.019	0.23	0.02	0.083	0.037	0.053	0.037

3.2. Experimental Test Setup

After explaining the numerical method it is time to perform experimental test and obtain the induced currents by these methods. When a linesmen is working under a TL (the position of the feet (0,y,z=0)) (Figure 5), based on [8], the most important electric field which effects its body is E_{1z}^{inc} (x=0,y,z=1) component. Therefore, these electric fields are considered for the experimental tests. The experimental test have been conducted for measuring the induced currents in the human organs (such as brain, heart, kidney and skin) when it is exposed to the electric fields (E_{1z}^{inc} (x=0,y=0:20,z=1)-Table 3) of a 200 kV TL at the various distances (0, 5, 10, 15, and 20 m) from the center of the tower (Figure 5).

For reaching to this goal, initially it is needed to fabricate a human body model. Two notes should be taken into account in this stage. First, the inside of the model should be empty for placing the human organs in it, therefore this model must not be made by conductive material and second, because the induced surface current is also measured, therefore the surface of this model should be conductive. Hence, based on the notes, as seen in Figure 6, a wooden human body model (the first note) (a 3-D test object) which can be covered by a layer of aluminum [1] (the second note) has been designed and fabricated. During measuring the induced currents of the human organs, the aluminum cover is removed from the surface of this model (Figure 6(a)), on the contrary, when the induced current of the surface is measured, a layer of aluminum cover (0Figure 6(b)) is put on the model.

TABLE 3.

THE VALUES OF E_{1z}^{inc} AND B_{1z}^{inc} NEAR THE HORIZONTALLY ARRANGED 200 kV TL (MAXIMUM VALUES)

	Z=1, m					
	V/m			μT		
Y, m	E_{1x}^{inc}	E_{1y}^{inc}	E_{1z}^{inc}	B_{1x}^{inc}	B_{1y}^{inc}	B_{1z}^{inc}
0	1.46×10^{-5}	86	94	0.189	0.3	0.39
5	6.04×10^{-5}	46	434	0.011	1.40	0.2
10	5.69×10^{-5}	9	523	0.0015	1.72	0.05
15	2.97×10^{-5}	22	416	0.0047	1.38	0.10
20	1.1×10^{-5}	18	289	0.0044	0.96	0.08
25	2.49×10^{-5}	12	195	0.0032	0.65	0.05
30	9.29×10^{-5}	8	134	0.0021	0.44	0.034

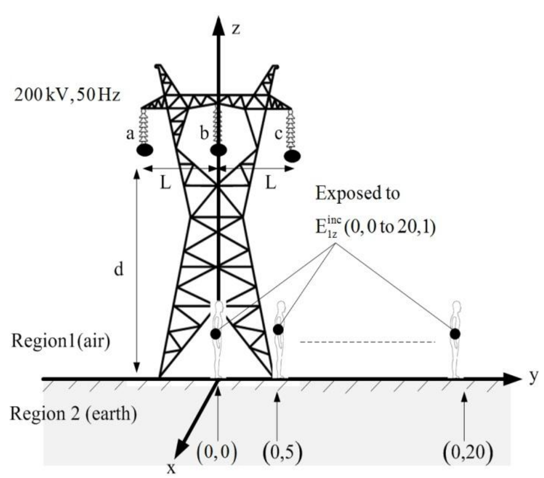

Figure 5. Three-phase HV transmission line horizontal arrangement (case study) (Table 1).

After designing and fabricating the human body model, it is the time to provide the human organs. Because the human organs are not easily accessible, sheep organs (brain, heart, and kidney) have been provided (Figure 7).

At the next step, equipment for producing the electric field of the 200 kV transmission line and also measuring the induced current should be provided. For creating the electric field and measuring the induced current, respectively, a metal rod as seen in Figure 8 and a digital scope digital including a voltage source and a computer as seen in Figure 9 have been chosen.

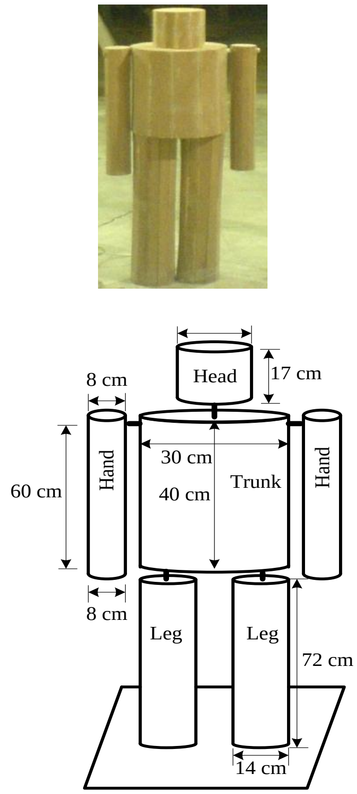

(a)

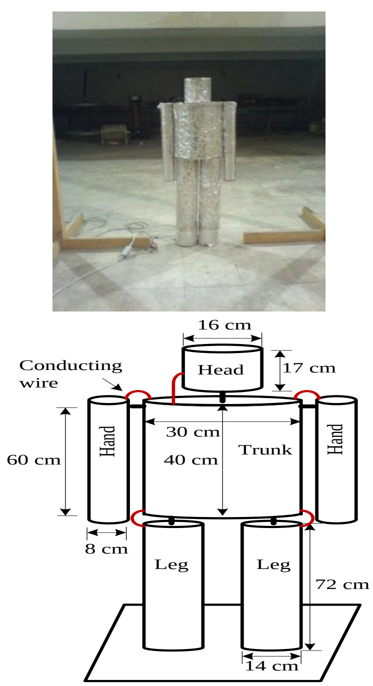

(b)

Figure 6. 3-Design and physical realization for measuring the induced currents of (a) the human organs, and (b) the surface of the human body.

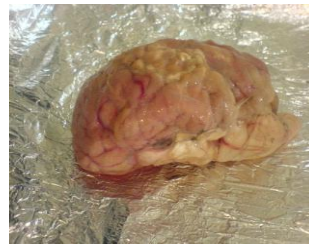

(a)

(b)

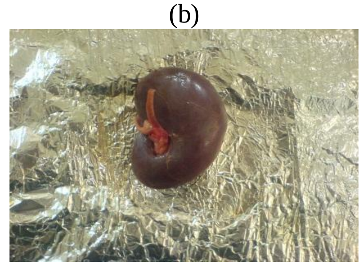

(c)

Figure 7. The under studied organs, (a) the brain 16 cm length, 6 cm width, and 4 cm height, (b) the heart 14 cm length, 5 cm width, and 3 cm height, (c) the kidney 7 cm length, 5 cm width, and 2 cm height.

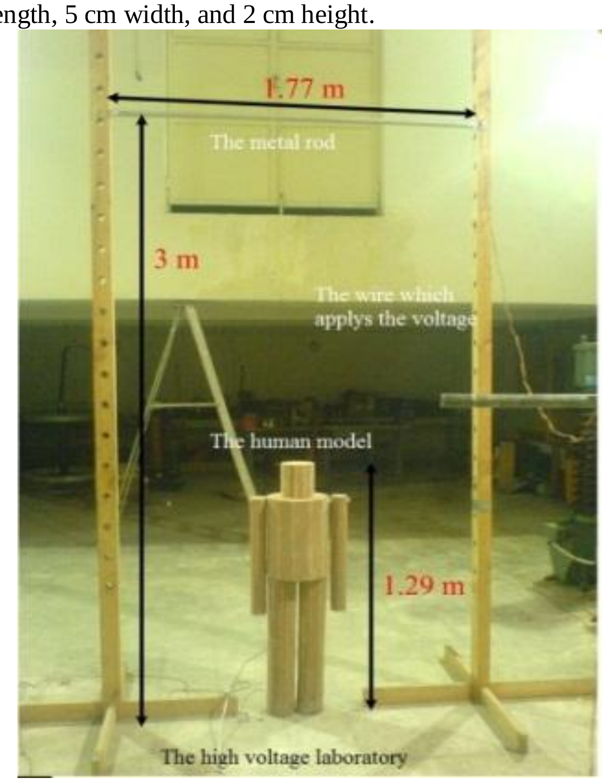

Figure 8. The experimental case study in the high voltage laboratory.

A 1.77 meter metal rod has been used for producing the electric field of the 200 kV transmission line (Table 2) in the laboratory. Therefore, it is needed to obtain the true voltages which should be applied to the metal rod for producing the exact electric fields of a 200 kV TL in the experimental test. The formula has been acquired by the Finite Element Method (FEM) (0Fig. 10). After calculation, the final equation is as (29).

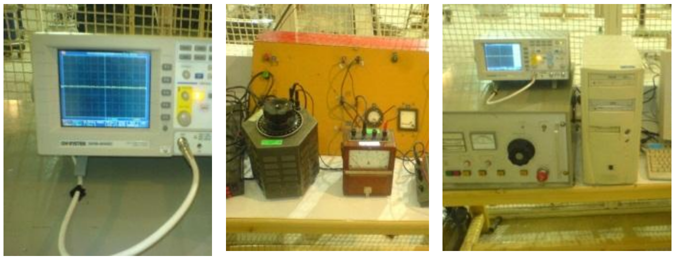
(a) (b) (c)

Figure 9. The required equipment, (a) the scope, (b) the voltage source, and (c) the computer.

After preparing the required equipment and calculating the values of the applied voltages, it is the time to obtain the induced currents. For measuring and observing the induced currents in the organs, they are placed in the human model in their real places and then the human model is located under the metal rod (Fig. 11, Fig. 13, Fig. 15, and Fig. 17) which has been energized by the power transformer at the calculated voltages (0Table 4). For observing the induced currents by the scope, each organ is connected to the earth by a resistance, and the across voltage of this resistance is measured which can be observed by the scope. Therefore, the induced current is calculated by dividing the across voltage to the value of the resistance (10.31 $M\Omega$).

$$V=-\frac{\rho_l}{4\pi\varepsilon_0}\left[\begin{array}{l}-\left(\ln\left(\dfrac{b+\sqrt{b^2+(z-3)^2}}{(z-3)}\right)\right)-\left(\ln\left(\dfrac{a+\sqrt{a^2+(z-3)^2}}{(z-3)}\right)\right)\\ +\left(\left(\ln\left(\dfrac{b+\sqrt{b^2+(z+3)^2}}{(z+3)}\right)\right)+\left(\ln\left(\dfrac{a+\sqrt{a^2+(z+3)^2}}{(z+3)}\right)\right)\right)\end{array}\right]_0^{3-r} \quad))$$

TABLE 4.
APPLIED VOLTAGES TO THE METAL ROD FOR PRODUCING THE ELECTRIC FIELD OF THE 200 kV TL IN THE LABORATORY

Y=Distance from the center of the tower (m)	0	5	10	15	20
Electric Field (V/m)	94	434	523	416	289
Applied voltage (kV) RMS	1.861	8.592	10.354	8.236	5.722

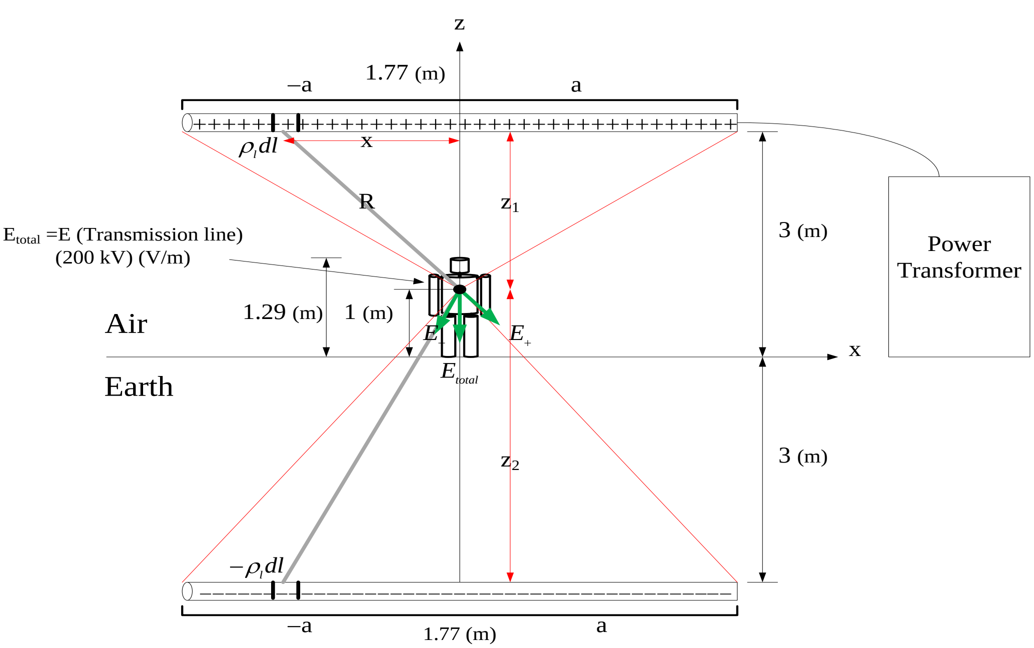

Figure 10. Applied voltage calculation for the metal rod.

4. RESULTS

In this section, the induced currents from the numerical method and the experimental test are obtained and compared to each other. The results are as follows:

- Brain experiment

When the rod metal is energized by the transformer for example at 1.86 kV (Table 4), it produces electric field around it; this electric field induces current in the brain that flows to the ground via the resistor (Fig. 11(b)). This current creates a voltage across the resistor as shown in Fig. 12(a). The induced current is obtained by dividing this voltage by the resistance value. The induced currents for 5 different applied voltages are obtained and compared by the simulation method in Table 5. These values should increase initially thanks to increasing the applied voltage and then decrease after 10 m because of decreasing the applied voltage, which can be seen in Fig. 12 and Table 5. This method for measuring the induced currents is similar for the rest of the experiments (Heart, kidney and feet).

- Brain experiment
- Heart experiment

The results obtaining from the scope are shown in Fig. 14. The results are compared in Table 6.

(a)

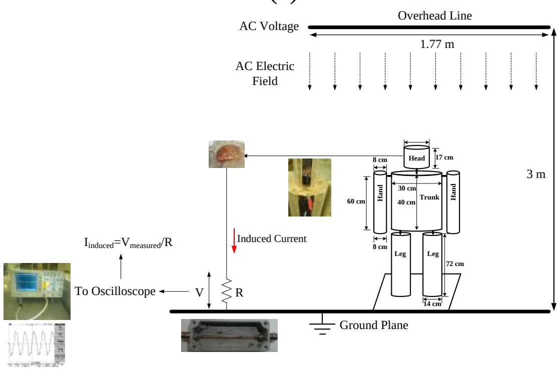

(b)

Figure 11. The brain experiment, (a) the place of the brain, (b) measuring the induced current.

- Kidney

The results obtaining from the scope are shown in Fig. 16. The results are compared in Table 7.

- **The surface of the body**

The results obtaining from the scope are shown in Fig. 18.
The results are compared in Table 8.
The compared results showed a good agreement between the numerical and the experimental results (the induced currents). Furthermore, the obtained results are lower than the critical values due to standard which are perilous to people's health [14].

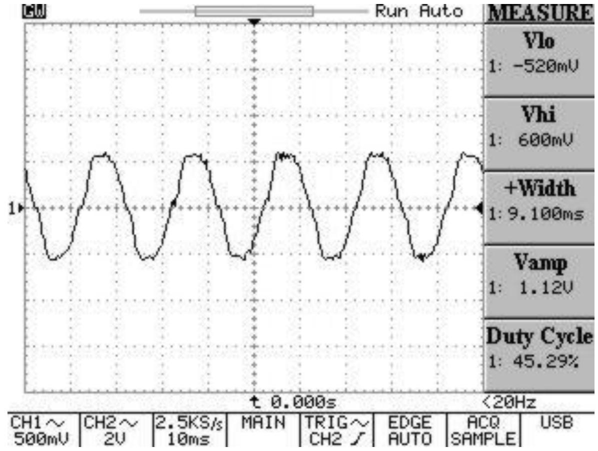

(a)

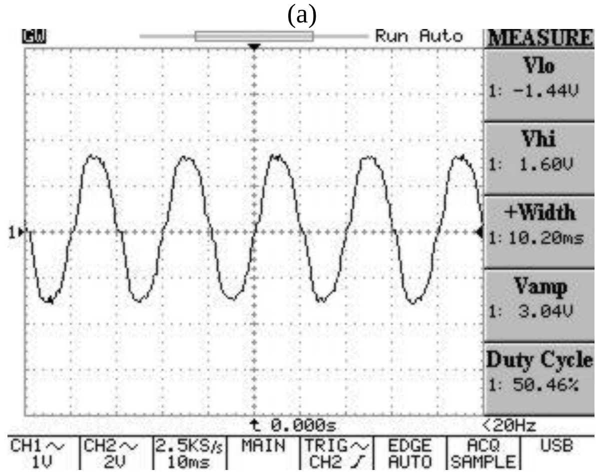

(b)

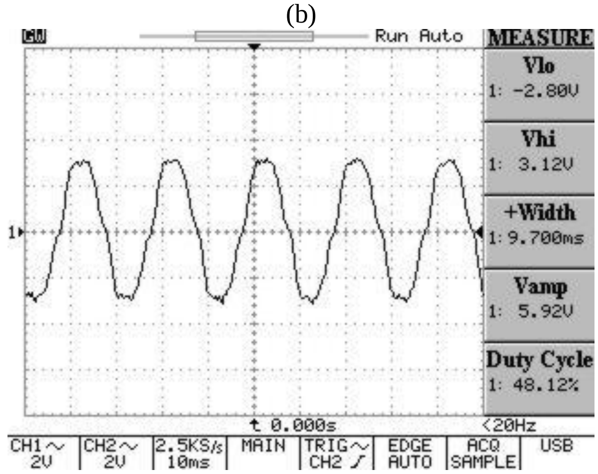

(c)

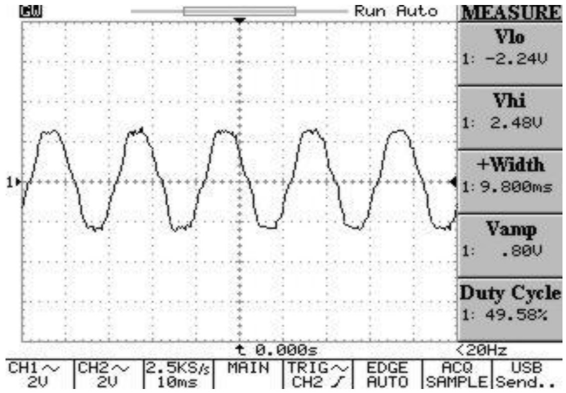

(d)

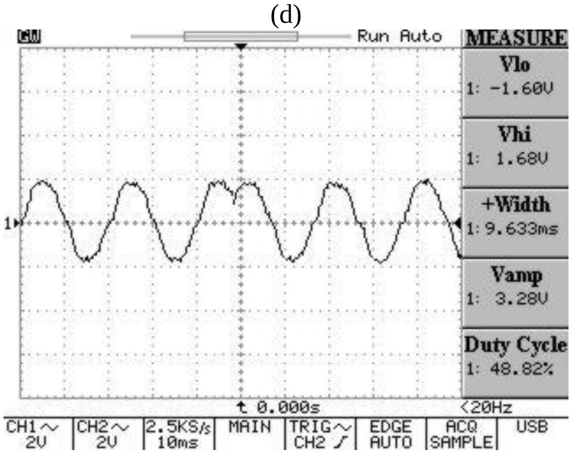

(e)

Figure 12. The voltages across the resistance, the distance from the center of the tower (m) (a) 0, (b) 5, (c) 10, (d) 15, and (e) 20.

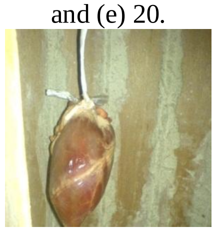

(a)

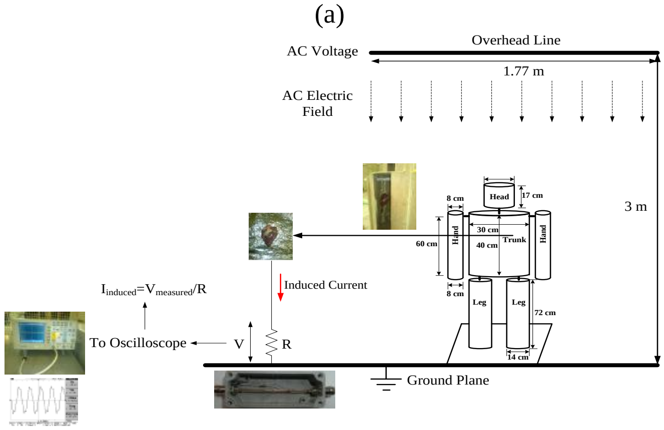

Figure 13. The heart experiment, (a) the place of it, and (b) measuring the induced current.

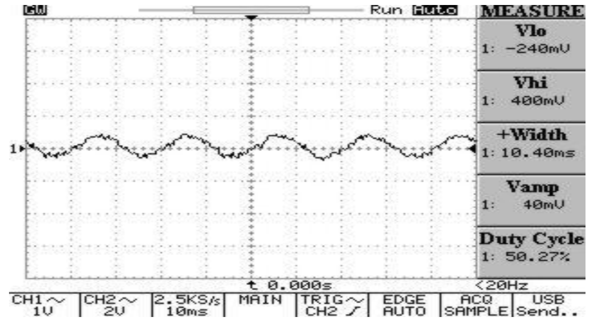

(a)

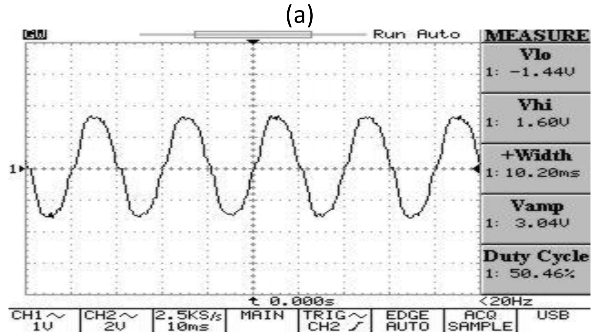

(b)

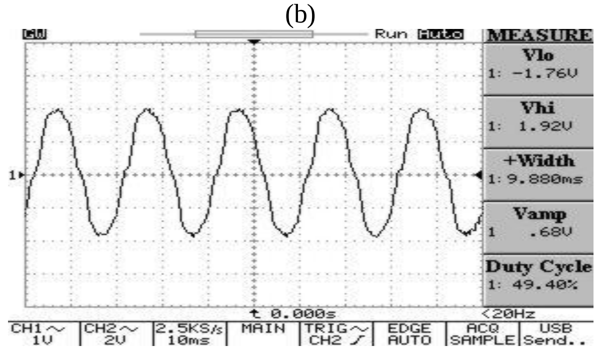

(c)

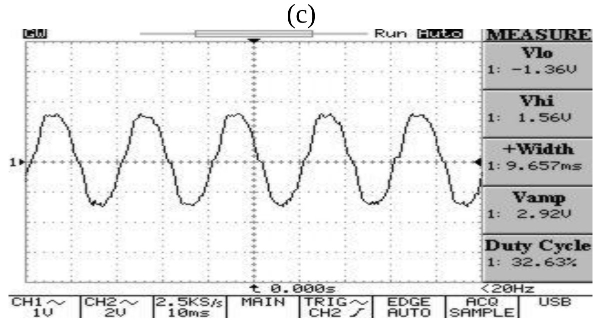

(d)

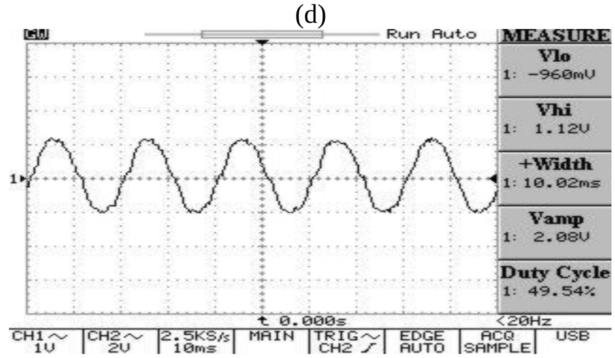

(e)

Figure 14. The voltages across the resistance, the distance from the center of the tower (m) (a) 0, (b) 5, (c) 10, (d) 15, and (e) 20.

TABLE 5.
THE INDUCED CURRENTS IN THE BRAIN, PRACTICAL AND SIMULATION RESULTS.

Y (m)	Applied Voltage (kV)	Induced Current (Practical-Test) (A)	Induced Current (Simulation-Numerical) (A)
0	1.861	4.12×10^{-8}	4.40×10^{-8}
5	8.592	1.76×10^{-7}	2.02×10^{-7}
10	10.354	2.14×10^{-7}	2.44×10^{-7}
15	8.236	1.70×10^{-7}	1.94×10^{-7}
20	5.722	1.15×10^{-7}	1.35×10^{-7}

TABLE 6.
THE INDUCED CURRENTS IN THE HEART, PRACTICAL AND SIMULATION RESULTS.

Y (m)	Applied Voltage (kV)	Induced Current (Practical-Test) (A)	Induced Current (Simulation-Numerical) (A)
0	1.861	2.74×10^{-8}	2.86×10^{-8}
5	8.592	1.10×10^{-7}	1.31×10^{-7}
10	10.354	1.32×10^{-7}	1.58×10^{-7}
15	8.236	1.07×10^{-7}	1.26×10^{-7}
20	5.722	7.68×10^{-8}	7.95×10^{-8}

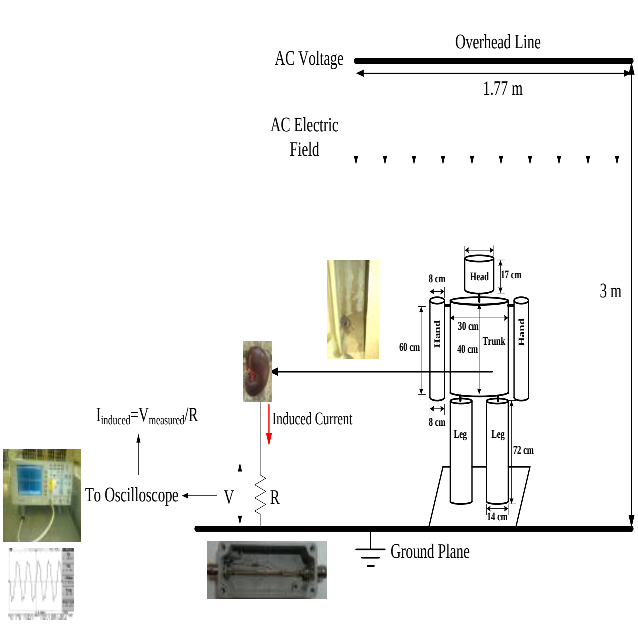

Figure 15. The kidney experiment, measuring the induced current.

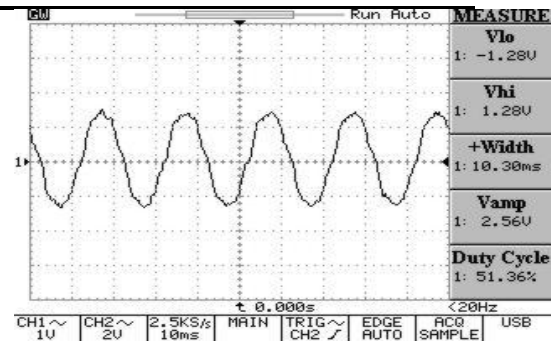

(b)

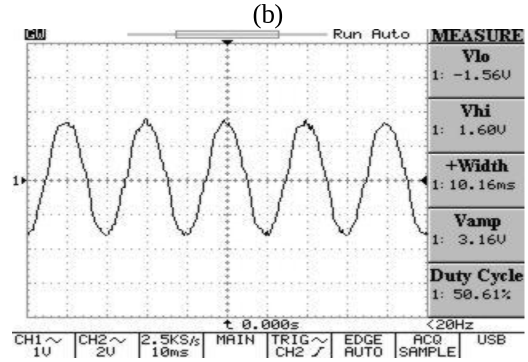

(c)

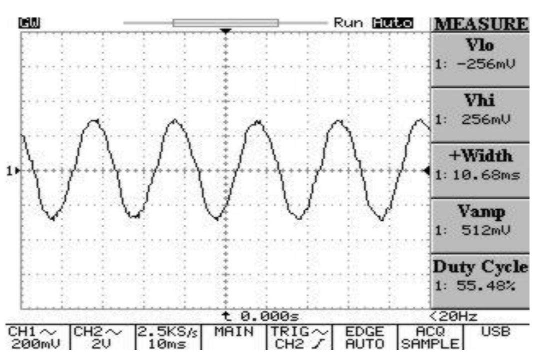

(a)

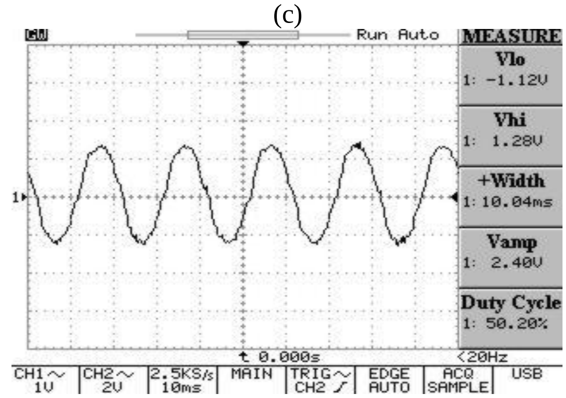

(d)

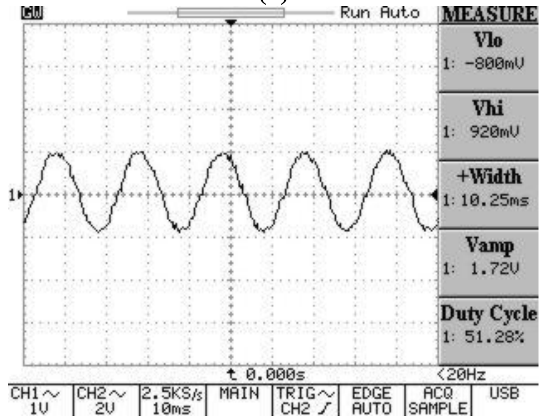

(e)

Figure 16. The voltage across the resistance, the distance from the center of the tower (m) (a) 0, (b) 5, (c) 10, (d) 15, and (e) 20.

TABLE 7.
THE INDUCED CURRENTS IN THE KIDNEY, PRACTICAL AND SIMULATION RESULTS.

Y (m)	Applied Voltage (kV)	Induced Current (Practical-Test) (A)	Induced Current (Simulation-Numerical) (A)
0	1.861	1.76×10^{-8}	1.95×10^{-8}
5	8.592	8.78×10^{-8}	9.12×10^{-8}
10	10.354	1.10×10^{-7}	1.36×10^{-7}
15	8.236	8.58×10^{-8}	9.10×10^{-8}
20	5.722	6.31×10^{-8}	6.69×10^{-8}

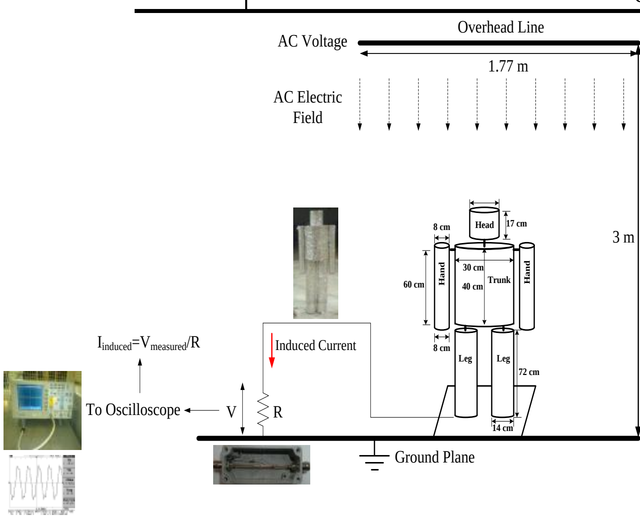

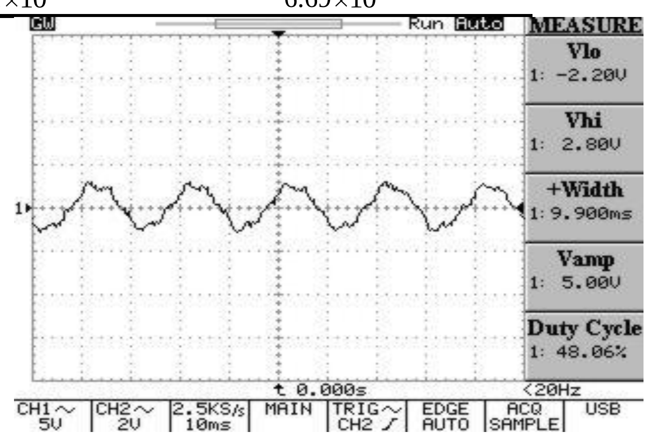

(a)

Figure 17. The surface experiment, measuring the induced current.

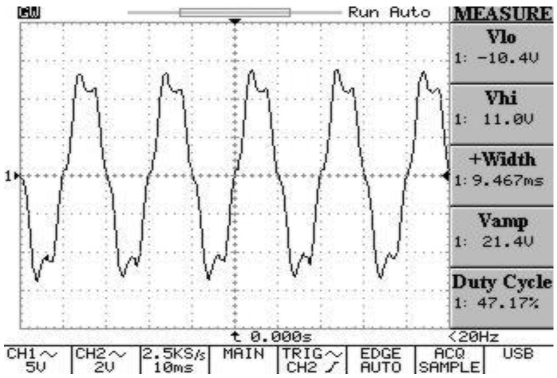

(b)

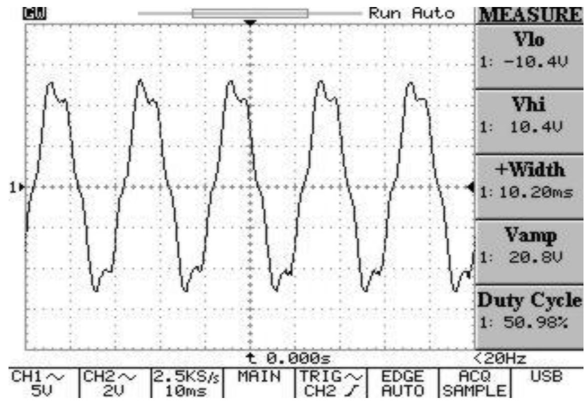

(d)

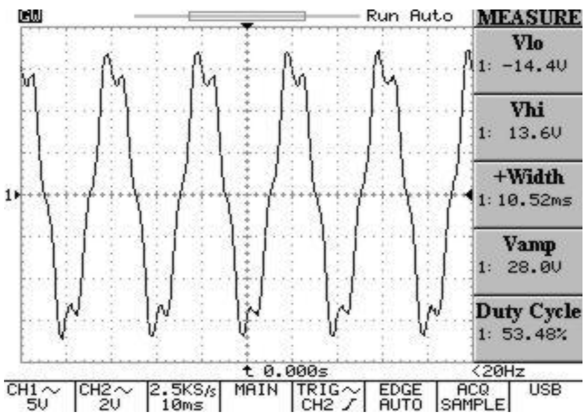

(c)

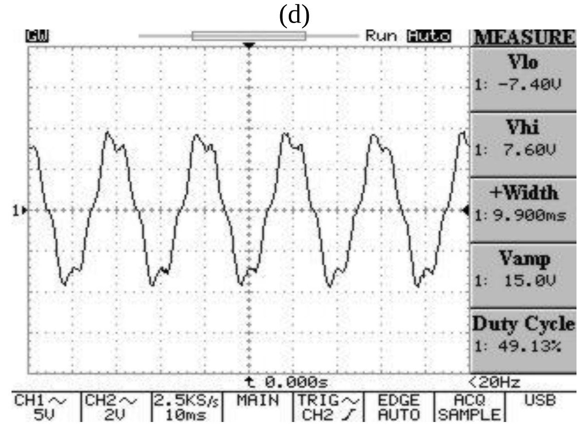

(e)

Figure 18. The voltage across the resistance, the distance from the center of the tower (m) (a) 0, (b) 5, (c) 10, (d) 15, and (e) 20.

TABLE 8.
THE INDUCED CURRENTS ON THE SURFACE, PRACTICAL AND SIMULATION RESULTS.

Y (m)	Applied Voltage (kV)	Induced Current (Practical-Test) (A)	Induced Current (Simulation-Numerical) (A)
0	1.861	1.92×10^{-7}	2.18×10^{-7}
5	8.592	1.06×10^{-6}	1.28×10^{-6}
10	10.354	1.31×10^{-6}	1.44×10^{-6}
15	8.236	1.00×10^{-6}	1.12×10^{-6}
20	5.722	7.37×10^{-7}	7.51×10^{-7}

From the paper it can be concluded that an EMF always exists when there is an electric current flowing in normal environment. A static EMF is naturally generated by earth and in case of direct current, and a man-made alternative magnetic field is produced by alternating current sources. Numerous investigations with EMF reported the alterations in cell, tissue and animal models. These reported changes have included alterations in endocrine and immune functions, developmental effect and biochemical metabolism. However, there has been a controversy on the biological effect of EMF because several studied has not been successfully replicated. Additionally, there have been no consistent evidences in human studies and epidemiological investigations. Despite the controversial results in laboratory and human studies, we are not able to ignore the ultimate biological effect of EMF including its health risk and therapeutic value. In the near future, a large number of laboratory studies and clinical application for therapeutic facilitators should be done to assess the real effect of EMF.

5. CONCLUSION

In this paper, the impact of the electric field of the 200 kV transmission line in the organs (brain, heart, and kidney) of a linesman and on the surface of it in the different distances have been investigated experimentally and numerically.

An efficient numerical technique for solving the Maxwell's equations with quasi-static approximations has been applied for calculating the induced currents when the human body is exposed to the incident electric field of the under studied TL in simulation.

For comprehending that the results obtained from the numerical method are true and accurate, an experimental test in the HV laboratory has been conducted. A human body model which its inside is empty for locating the organs in has been fabricated by wood because the body must not be conductive. But on the contrary, when the induced current on the surface is measured, a layer of aluminum is covered on it.

The compared results revealed a good agreement between the numerical results and the experimental results. Moreover, the obtained results (the induced currents) are lower than the critical values due to standard which are perilous to people's health.

REFERENCES

[1] Ahmed, Y. Rowland, S. M. "Modelling Linesmen's Potentials in Proximity to Overhead Lines", *IEEE Transaction on Power Delivery*, **24**(4): 2270-2275 (2009).

[2] Garrido, C. Otero, A. F. Cidras, J. "Low-frequency Magnetic Fields From Electrical Appliances and Power Lines", *IEEE Transaction on Power Delivery*, **18**(4): 1310-1319 (2003).

[3] Korobkova, V. P. Morozov, Y. A. Stolarov, M. D. Yakub, Y. A. "Influence of the Electric Field in 500 kV and 750 kV Switchyards on Maintenance Staff and Means for Its Protection", *Technical Report 23-06, CIGRE paper*, 1972.

[4] Reilly, J. P. Delapace, L. R. "Electric and Magnetic Field Coupling from High Voltage ac Power Transmission Lines-Classification of Short-Term Effects on People, "*IEEE Transaction on Power Apparatus and System*, **PAS-97**(6): 2243–2252 (1978).

[5] Christ, A. Kainz, W. Hahn, E. Janka, R. Bautz, W. Kiefer, B. Schmitt, P. Hollenbach, H. P. Kam, A. Neufeld, E. Oberle, M. Kuster, N. "The Virtual Family Project-Development of Anatomical Whole-Body Models of Two Adults and Two Children", *Proceedings of the 23rd Annual Review of Progress in Applied Computational Electromagnetics* (ACES), 2007

[6] Brenner, S. C. Scott, R. "The Mathematical Theory of Finite Element Methods", Texts in Applied Mathematics, Brenner, Ridgway 3rd edition, 2008.

[7] King, R. W. P. Wu, T. T. "The Complete Electromagnetic Field of a Three-phase Transmission Line over the Earth and Its Interaction with the Human Body", *Journal of Applied Physics*, **78**(2): 668-683 (1995).

[8] King, R. W. P. "Fields and Currents in the Organs of the Human Body When Exposed to Power Lines and VLF transmitters," *IEEE Transactions on Biomedical Engineering*, **45**(4): 520–530 (1998).

[9] Hara, M. Wada, T. Fukasawa, T. Kikuchi, P. "A Three Dimensional Analysis of RF Electromagnetic Fields by the Finite Element Method", *IEEE Transaction on Magnetic*, **MAG-19**(6): 2417-2420 (1983).

[10] Xu X. B. Yang, X. M. "A Simple Computational Method for Predicting Magnetic Fields in the Vicinity of three-phase Underground Cable with a Fluid-Filled Steel-Pipe Enclosure", *IEEE Transaction on Power Delivery*, **10**(1): 78-84 (1995).

[11] Olsen, R. G. Lyon, C. E. "Modeling of Extremely Low Frequency Magnetic Field Sources Using Multi-pole Techniques", *IEEE Transaction on Power Delivery*, **11**(3): 1563-1570 (1996).

[12] Satsios, K. J. Labridis, D. P. Dokopoulos, P. S. "Finite Element Computation of the Field and Eddy Currents of a System Consisting of a Power Transmission Line Above Conductors Buried in Nonhomogeneous Earth", *IEEE Transaction on Power Delivery*, **13**(3): 876-882 (1998).

[13] Carson, J. R. "Wave Propagation in Overhead Wires with Ground Return", *Bell System Technical Journal*, **5**(4): 539-554 (1926).

[14] Transmission Line Reference Book. 345 kV and Above, 2nd ed. Palo Alto, CA: Electric Power Research Institute (EPRI), 1987.

[15] Plonus, M. A. "Applied Electromagnetics", New York: McGraw-Hill, 1978.

[16] Hoang, L. H. Scorretti, R. Burais, N. Voyer, D. "Numerical Dosimetry of Induced Phenomena in the Human Body by a Three-Phase Power Line", *IEEE Transaction on Magnetics*, **45**(3): 1666-1669 (2009).

[17] Huebner, K. H. Dewhirst, D. L. Smith, D. E. Byrom, T. G. "The Mathematical Theory of Finite Element Methods", John Wiley & Sons, Inc, 24th August 2001.

[18] Gabriel, S. Lau, R. W. Gabriel, C. "The Dielectric Properties of Biological Tissues: Measurements in the Frequency Range 10Hz to 20GHz", *Physics in Medicine and Biology*, **41**(11): 2251-2269 (1996).

[19] Krajewski, W. "Numerical Assessment of Electromagnetic Exposure during Live-line Works on High-voltage Objects", *IET Science, Measurement & Technology*, **3**(1): 27-38 (2009).